The Astrophysical Journal, 713:66–81, 2010 April 10 doi:10.1088/0004-637X/713/1/66

HUBBLE SPACE TELESCOPE NEAR-INFRARED SNAPSHOT SURVEY OF 3CR RADIO SOURCE COUNTERPARTS. III. RADIO GALAXIES AND QUASARS IN CONTEXT*

David J. E. Floyd[1,8], David Axon[2,3], Stefi Baum[2], Alessandro Capetti[4], Marco Chiaberge[1,5], Juan Madrid[1,6], Christopher P. O'Dea[2], Eric Perlman[7], and William Sparks[1]
[1] Space Telescope Science Institute, 3700 San Martin Drive, Baltimore, MD 21218, USA; dfloyd@unimelb.edu.au
[2] Department of Physics, Rochester Institute of Technology, 84 Lomb Memorial Drive, Rochester, NY 14623, USA
[3] School of Mathematical & Physical Sciences, University of Sussex, Falmer, Brighton, BN2 9BH, UK
[4] INAF–Osservatorio Astronomico di Torino, Via Osservatorio 20, I-10025 Pino Torinese, Italy
[5] INAF–IRA, Via P. Gobetti 101, I-40129 Bologna, Italy
[6] Centre for Astrophysics & Supercomputing, Swinburne University of Technology, P.O. Box 218, Hawthorn, VIC 3122, Australia
[7] Florida Institute of Technology, Physics & Space Sciences Department, 150 W. University Blvd., Melbourne, FL 32901, USA
Received 2009 November 27; accepted 2010 February 22; published 2010 March 17

ABSTRACT

We compare the near-infrared (NIR) *H*-band photometric and morphological properties of low-z ($z < 0.3$) 3CR radio galaxies with samples of BL Lac objects and quasar host galaxies, merger remnants, quiescent elliptical galaxies, and brightest cluster galaxies drawn from the literature. In general, the 3CR host galaxies are consistent with luminous ($\sim L^{\star}$) elliptical galaxies. The vast majority of FR II's ($\sim$80%) occupy the most massive ellipticals and form a homogeneous population that is comparable to the population of radio-loud quasar (RLQ) host galaxies in the literature. However, a significant minority ($\sim$20%) of the 3CR FR II's appears under-luminous with respect to quasar host galaxies. All FR II objects in this faint tail are either unusually red, or appear to be the brightest objects within a group. We discuss the apparent differences between the radio galaxy and RLQ host galaxy populations. RLQs appear to require $\gtrsim 10^{11}\ M_{\odot}$ host galaxies (and $\sim 10^{9}\ M_{\odot}$ black holes), whereas radio galaxies and radio-quiet quasars can exist in galaxies down to $\sim 3 \times 10^{10}\ M_{\odot}$. This may be due to biases in the measured quasar host galaxy luminosities or populations studied, or due to a genuine difference in host galaxy. If due to a genuine difference, it would support the idea that radio and optical active galactic nuclei are two separate populations with a significant overlap.

Key words: galaxies: active – galaxies: fundamental parameters – quasars: general

1. INTRODUCTION

Much effort has been invested over the last decade and a half to characterize the host galaxies of quasars using the *Hubble Space Telescope* (*HST*). Unfortunately by their very nature quasars remain difficult to study, and results remain ambiguous due to selection effects. Detailed isophotal analysis of quasar host galaxies is impossible due to the strongly anisotropic contamination by the nucleus and the point-spread function (PSF) of the instrument, which also hinder accurate spectroscopy and thus measurement of host galaxy dynamics. In the absence of any forthcoming space-based coronographic mission (e.g., the Terrestrial Planet Finder Coronograph—TPF-C[9]), researchers have begun to explore the nature of type 2 (heavily obscured) active galactic nuclei (AGNs) to study their environments in greater detail (e.g., Zakamska et al. 2006). Type 2 AGNs have been identified from the Sloan Digital Sky Survey (SDSS) out to $z = 0.83$ (Zakamska et al. 2003), but the sample remains incomplete and biases difficult to measure. Radio galaxies offer us an alternative sample of type 2 radio-loud AGN, detectable to far higher redshifts in a statistically complete manner.

In this paper, we compare the overall near-infrared (NIR; *H* band) galaxy properties of the $z < 0.3$ 3CR radio galaxies with those of quasars and BL Lac objects at similar redshift, and to quiescent early-type galaxies and mergers available in the literature. For the reasons outlined above, we intend to use the radio galaxies as a link or bridge between the quasars and quiescent galaxies which can be studied in much greater structural, dynamical, and population detail. Nearby radio galaxies have been statistically studied in recent papers (Best et al. 2005; Mauch & Sadler 2007) and are well-known to occupy luminous galaxies in general. Indeed it is by now accepted that the primary requirement for radio-loud AGN activity is a supermassive black hole $\gtrsim 10^{9}\ M_{\odot}$, which generally requires a very luminous elliptical host galaxy. The principal aim of this paper is to explore in detail the subset of galaxies drawn from the nearby universe that are capable of hosting a radio-loud AGN. We wish to determine what additional effects the host galaxy plays in determining the radio loudness of a source, and to identify any sources that are hosted by "unusual" galaxies. A secondary aim is to determine whether there are any systematic biases introduced in the study of quasar host galaxies.

Our approach is to analyze the results of isophotal and parametric modeling of the host galaxies of 3CR radio sources from Madrid et al. (2006, hereafter Paper I), and Floyd et al. (2008, hereafter Paper II), and to compare the results to those for similarly studied samples of galaxies and AGNs. In Paper I, we presented the imaging and photometry for the first part of our survey. In Paper II, we presented the modeling used here, and showed that two different techniques (widely adopted by the galaxy morphology and quasar host galaxy communities, respectively) reliably recovered the properties of the NIR host

* Based on observations with the NASA/ESA *Hubble Space Telescope*, obtained at the Space Telescope Science Institute, which is operated by the Association of Universities for Research in Astronomy, Inc. (AURA), under NASA contract NAS5-26555.
[8] AAO/OCIW Magellan Fellow. Current address: School of Physics, University of Melbourne, Victoria 3010, Australia.
[9] http://planetquest.jpl.nasa.gov/TPF-C/tpf-C_index.cfm

galaxies of the low-redshift ($z < 0.3$) 3CR radio sources without strong optical nuclei. Furthermore, for synthetic quasars (created by taking a true galaxy and adding an artificial central point source), the quasar modeling technique was shown to recover the correct underlying morphological parameters to within 10%, and galaxy luminosity within to 2%.

The galaxies associated with the 3CR radio sources have long been known to be typically elliptical (Matthews et al. 1964), with a number of them associated with the brightest galaxies in a cluster or group (Burns 1990; Best et al. 2007). Recent surveys with *HST* have revealed a wealth of information on the environments of these uniquely powerful sources at a range of wavelengths (de Koff et al. 1996, 2000; Martel et al. 1999; Allen et al. 2002; Madrid et al. 2006; Privon et al. 2008; Floyd et al. 2008), and uncovered numerous new jets, dust disks, etc. But until recently (Donzelli et al. 2007; Floyd et al. 2008), the 3CR lacked a detailed and systematic classification of their host galaxies in such a way that can be straightforwardly compared with existing samples of quiescent galaxies in the literature. Observing in the infrared offers important advantages in the study of both galaxies and AGNs providing a direct measure of dynamically dominant old stellar population, an almost-constant mass-to-light ratio (Zibetti et al. 2002), and a peak in the ratio of galaxy to AGN continuum, giving the best chance of detecting the host galaxy in cases where the AGN is unobscured. Thus, it seems a natural application of the NICMOS *H*-band data set to make a direct comparison to similar samples in the literature. We need to be certain which radio galaxies correspond to which radio-loud quasars (RLQs) in order to be able to use radio galaxies as a proxy for quasars in detailed spectroscopical, dynamical, and structural studies of the effect of AGN on environment and vice versa.

This paper is structured as follows. In Section 2, we describe the samples used in this paper, and refer briefly to the observations and data reduction used. In Section 3, we describe the results of sample-wide comparisons according to different observational properties of the galaxies. In Section 4, we discuss those comparisons, property-by-property across all the samples studied, and look at the R_e–μ_e Kormendy relation, host-to-nuclear luminosity distribution, and host luminosity versus extended radio power distributions. We pick out several anomalously faint 3CR host galaxies for discussion in further detail in Section 5. In Section 6, we attempt to draw this discussion together and look at the issues remaining in the study of quasar host galaxies. Finally, we conclude in Section 7 with a summary of our findings and suggestions for future study.

2. SAMPLES, OBSERVATIONS, AND DATA REDUCTION

In this paper, we take the revised 3C sample (3CR) as defined by Spinrad et al. (1985), restricted to $z < 0.3$, as a statistically complete sample of low-redshift radio galaxies, and compare it in various physical terms with samples of low-redshift quasars, quiescent galaxies, and mergers that have deep imaging and structural modeling of the galaxies available in the literature. The 3CR covers sources in the northern hemisphere that are brighter than 9 Jy at 178 MHz. *H*-band snapshot observations of the low-z 3CR sample (as defined by Spinrad et al. 1985) began in *HST* Cycle 13, using NICMOS 2; and we presented the first year's imaging in Paper I. Observations continued through Cycle 14 yielding a total of 101 sources (an 87% completeness), including 11 drawn from the NICMOS 2 archive. Modeling and classification of all 101 galaxies were presented in Paper II. In the present paper, we revisit those modeling results, drawing comparisons with other galaxy samples drawn from the literature. See Paper I for full details of the 3CR NIC2 observations and notes on half the sample. See Paper II for details of the 3CR NIC2 data reduction, modeling results, and notes on the remainder of the sample. In particular, the machine-readable Tables 3–5 of Paper II contain the basic radio properties, one-dimensional and two-dimensional Sérsic profile fits, respectively, for the entire present sample of 101 3CR sources. Also see Jenkins et al. 1977 and Giovannini et al. 1988 for 5 GHz radio properties, and Lilly & Longair (1984) for *K*-band fluxes. All reduced, science ready data is available for public download from the STScI archive Web site.[10]

Note that from the original sample modeled in Paper II, we omit 3C 258 from study in this paper because, as discussed in Paper II, it is found to be a higher redshift ($z \gtrsim 1$) RLQ located behind a $z = 0.165$ irregular galaxy.

2.1. Cosmology, Photometry, and Evolution

We throughout assume a flat, Λ-dominated cosmology in which $\Omega_\Lambda = 0.7$, and $h_0 = 0.7$. For each source, we have *k*-corrected the apparent magnitudes to rest-frame *H* band assuming a spectral index of $\alpha = 1.5$ for the host galaxy and $\alpha = 0.2$ for the nucleus where necessary ($f_\nu \propto \nu^{-\alpha}$). Galactic extinction corrections have been applied following Schlegel et al. (1998). Comparison samples have been converted to the rest-frame wavelength (and correct angular diameter distance) of our study following the same cosmological assumptions and using a throughput template for the NICMOS2 F160W (*H*-band) filter and the appropriate filter/instrument configuration for the original observations.

Note that few samples exist to precisely match our redshift distribution. Out to $z = 0.3$, we are probing a total look-back time of 3.4 Gyr. While evolution is not negligible across such a time frame, on the basis of our hypothesis that the 3CR represent a subsample of the most massive elliptical galaxies at low redshift, it is safe to assume that most of the mass has formed much earlier and that now the galaxies are evolving more-or-less passively. The radio sources themselves will have evolved significantly, but again, following our null hypothesis, all early-type galaxies should have hosted a radio source at some point over this epoch. For quasars, we can construct samples that span a similar redshift range, while for quiescent galaxies existing morphological studies tend to concentrate on local samples, but it is informative to compare with quiescent galaxy samples where they are available.

2.2. Comparison Samples

We explored the literature for suitable samples with comparable published data—morphological information from one- or two-dimensional fitting. We take BL Lac objects and quasars with deep imaging and well-studied host galaxies from the samples of Taylor et al. (1996); Urry et al. (2000); McLeod & McLeod (2001); Dunlop et al. (2003); and Floyd et al. (2004). Quiescent early-type galaxies are taken from Bender et al. (1992); Pahre (1999); Mobasher et al. (1999); and Ferrarese et al. (2006). Merger remnants we take from Rothberg & Joseph (2004). Finally, we use the brightest cluster galaxy (BCG) sample studied by Graham et al. (1996). The samples in each of these papers are briefly discussed below. See Table 1 for basic details of the comparison samples at a glance.

[10] http://archive.stsci.edu/prepds/3cr/

Table 1
Details of the Comparison Samples Used in this Paper

Reference	Sample Type	N_s[a]	Telescope/Instrument	Filter	Sample Distance	Selection Notes
U+00[b]	BL Lac object	30	*HST*/WFPC2	*R*	$0.0 < z < 1.3$	Composite sample; 30 sources at $z < 0.3$
MM01[c]	RQQ	16	*HST*/NICMOS2	*H*	$z \approx 0.3$	Luminous QSOs at $z < 0.3$
D+03[d]	RLQ, RQQ, RG	33	*HST*/WFPC2	*R*	$z = 0.2$	Optically matched samples of RLQ and RQQ
F+04[e]	RLQ, RQQ	17	*HST*/WFPC2	*I*	$z = 0.4$	Optically luminous QSOs
T+96[f]	RLQ, RQQ, RG	33	UKIRT/IRCAM	*K*	$z = 0.2$	We use D+03[d] subsample
RJ04[g]	Merger	51	U. Hawaii 2.2 m/QUIRC	*K*	$z < 0.045$	Single-nucleus candidate disk-merger remnants
BBF92[h,i]	Elliptical	80	Calar-Alto 1.23 m	*V*, *R*, *I*	$D < 140$ Mpc	Nearby *B*-band luminous ellipticals
P99[j]	Elliptical	341	Palomar 60 inch; LCO 1 m, 2.5 m	*K*	$z < 0.03$	Various nearby galaxies, groups, and clusters
M+99[k]	Elliptical	48	UKIRT/IRCAM3	*K*	$\bar{D} = 99$ Mpc	Coma cluster ellipticals
F+06[l]	Early type	100	*HST*/ACS-WFC	*g*, *z*	$\bar{D} = 18$ Mpc	Virgo cluster early types
G+96[m,n]	BCG	119	CTIO 1.5 m; KPNO 2.1 m, 4 m	*R*	$0.01 < z < 0.054$	Abell brightest cluster galaxies
I, II[o,p]	RG	101	*HST*/NICMOS	*H*	$z < 0.3$	Present study

Notes.
[a] Sample size used.
References.
[b] Urry et al. 2000.
[c] McLeod & McLeod 2001.
[d] Dunlop et al. 2003.
[e] Floyd et al. 2004.
[f] Taylor et al. 1996.
[g] Rothberg & Joseph 2004.
[h] Bender et al. 1992.
[i] Bender & Moellenhoff 1987.
[j] Pahre 1999.
[k] Mobasher et al. 1999.
[l] Ferrarese et al. 2006.
[m] Graham et al. 1996.
[n] Postman & Lauer 1995.
[o] Madrid et al. 2006.
[p] Floyd et al. 2008.

In each case, we have taken care to compare published properties with equivalent properties within our sample. A wide range of conventions are used in the literature for describing scale length, surface brightness, and diskiness. We have made use of the conversions discussed by Milvang-Jensen & Jørgensen (1999). In cases where the total magnitude of the (modeled) host galaxy was unavailable, we have calculated it from the basic model parameters using the prescriptions in the same paper.

Note that, at present, there are insufficient quasars and BL Lac objects with observed host galaxies to produce a complete or volume-limited sample. The radio luminosity–redshift distributions are compared in Figure 1. The 178 MHz luminosity distribution of the combined radio-loud QSO+BL Lac object sample forms a good match to that of the 3CR, with a Kolmogorov–Smirnov (K–S) test returning $D = 0.20$, with $p = 0.76$, indicating no significant differences between the radio power distributions of the two samples.

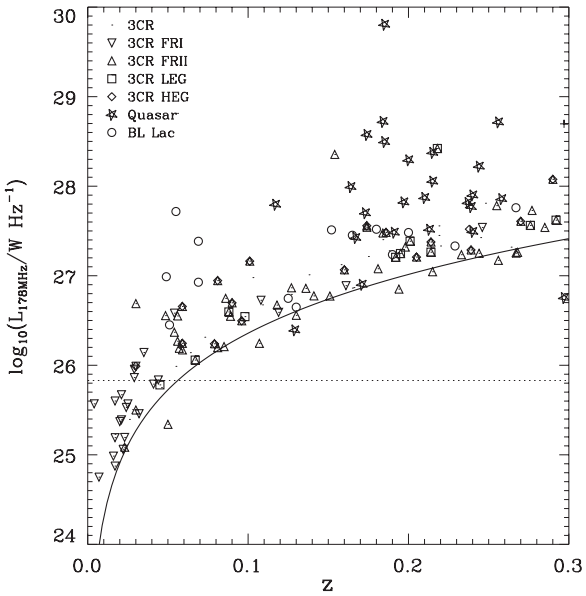

Figure 1. Rest-frame 178 MHz radio luminosity of the present sample (down-pointing triangles = FR I's; up-pointing triangles = FR II's; diamonds = HEGs; squares = LEGs), along with the quasars (stars) and BL Lac objects (circles) with radio detections from Urry et al. (2000); McLeod & McLeod (2001); Dunlop et al. (2003); and Floyd et al. (2004). The dotted line shows the radio-quiet cutoff traditionally adopted in quasar studies ($\log_{10}(L_{178}) = 25.83$). The 3CR definition is of sources brighter than 9 Jy at 178 MHz.

2.2.1. Quasars and BL Lac objects

Urry et al. (2000). Urry et al. (2000) obtained *HST*/WFPC2 F702W (*R*-band) images of 110 BL Lac objects drawn from a 132 strong sample at $0 \lesssim z \lesssim 1.3$. The sample is a composite of seven complete catalogs selected in the radio, X-ray, and optical. We use only those 30 sources that fall into the redshift range of our sample ($0.0 < z < 0.3$). Urry et al. apply a one-dimensional fit to an azimuthally averaged radial profile of the source, simultaneously fitting both host and nucleus. They adopt an exponential disk, and a de Vaucouleurs $R^{1/4}$ law, but do not fit Sérsic models, nor ellipticities. As part of a survey of QSO hosts in the *HST* archive (D. J. E. Floyd et al. 2010, in preparation), we have refit the Urry et al. host galaxies with a Sérsic model, using the same technique as described in Floyd et al. (2004) and Paper

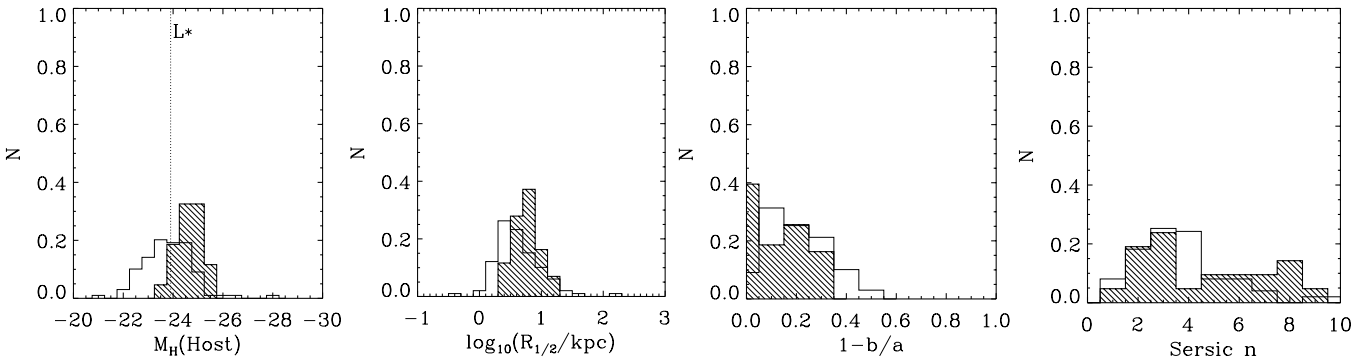

Figure 2. Histograms for the present 3CR sample (open) and the Urry et al. (2000) BL Lac object sample (shaded) for the following properties (from left to right): host galaxy luminosity (converted *H* band); scale length; ellipticity; Sérsic index. $L^{\star}$ is indicated by a dotted line on the left-hand figure. The results of a two-sided K–S test for each distribution are presented in Table 2.

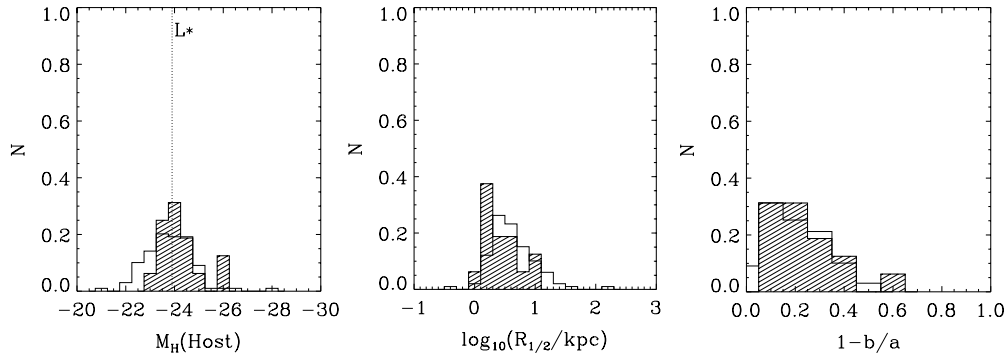

Figure 3. Histograms for the present 3CR sample (open) and the McLeod & McLeod (2001) RQQ sample (shaded) for the following properties (from left to right): host galaxy luminosity (converted to *H* band); scale length; ellipticity. $L^{\star}$ is indicated by a dotted line on the left-hand figure. The results of a two-sided K–S test for each distribution are presented in Table 2.

II. We use these results (which are consistent in terms of host luminosity with the original data) to compare Sérsic parameters. See Figure 2 for a comparison of the Urry sample with the 3CR.

McLeod & McLeod (2001). McLeod & McLeod (2001) studied 16 $z \approx 0.3$ optically luminous radio-quiet quasar (RQQ) host galaxies in the NIR F160W filter (*H* band) using NICMOS. The authors adopted a PSF-subtraction technique, followed by modeling of the residual host galaxy using both one-dimensional and two-dimensional analysis. We compare our two-dimensional results to their two-dimensional results which fit exponential disk and de Vaucouleurs elliptical models, but no Sérsic profile. Due to the presence of saturated cores in almost all of the images, we were unable to remodel this data using our technique. Figure 3 shows the various properties of the sample compared with those of the 3CR.

Dunlop et al. (2003) and Taylor et al. (1996). Dunlop et al. (2003) studied the largest and most stringently selected sample of low-redshift quasars: 10 RLQs, 13 RQQs, and 10 radio galaxies at $z \approx 0.2$. The RLQ and RQQ subsamples were optically matched, and the RLQs and radio galaxies were matched in terms of their radio luminosities. The sample selection avoided core-dominated radio sources in order to minimize the chances of beaming producing artificially boosted apparent radio luminosities. Targets were observed using *HST*/WFPC2 with the F675W (*R*-band) filter. Figure 4 illustrates the various properties of the sample compared with those of the 3CR. The same objects were previously observed from the ground using UKIRT/IRCAM in *K* band by Taylor et al. (1996)—see Figure 5.

Floyd et al. (2004). Floyd et al. (2004) studied the host galaxies of 17 quasars at $z \approx 0.4$ (including those of the seven optically brightest QSOs at $z < 0.4$) using *HST*/WFPC2 F814W (*I*-band) imaging. The lower luminosity subsample (10 objects) was divided into equal-sized subsamples of RLQs and RQQs that are optically matched both with each other and with the sample of Dunlop et al. (2003). Similar care was taken to avoid beamed radio sources as in the Dunlop sample. Figure 6 shows the various properties of the sample compared with those of the 3CR.

2.2.2. Mergers

Rothberg & Joseph (2004). Rothberg & Joseph (2004) studied a sample of 51 nearby ($z < 0.045$) candidate disk-merger remnants, all with a single nucleus, and based on optical morphologies to include objects with tidal loops, tails, and shells. The study used ground-based *K*-band data and one-dimensional radial profile fitting to elliptical isophotal values in the same way as our one-dimensional approach. Observations were taken using QUIRC at $f/10$ on the University of Hawaii 2.2 m telescope. This is the only large sample or mergers that has been studied in such morphological detail to date. Figure 7 shows the Rothberg sample compared to the 3CR. Figure 8 shows the Rothberg sample compared to only those 3CR sources that were flagged as mergers in Paper II.

2.2.3. Elliptical and Early-type Galaxies

Bender et al. (1992). Bender et al. (1992) studied a sample of local ($D < 140$ Mpc) "dynamically hot galaxies," that are in practice a range of spheroids and bulges selected in terms of their *B*-band luminosity. The sample includes 48 giant ellipticals (defined as having $M_B \leqslant -20.5$), 20 intermediate

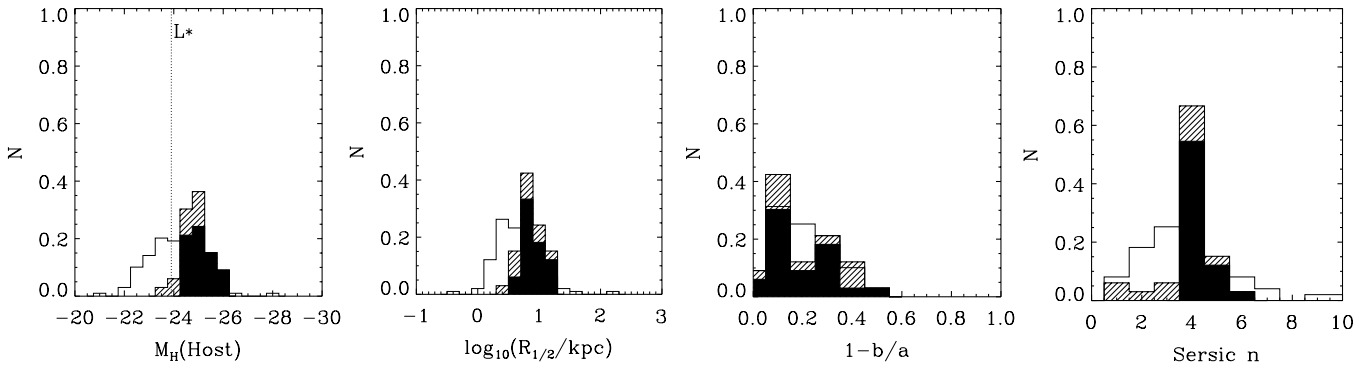

Figure 4. Histograms for the present 3CR sample (open) and the Dunlop et al. (2003) quasar sample (full sample—shaded; RLQs—black) for the following properties (from left to right): host galaxy luminosity (converted *H* band); scale length; ellipticity; Sérsic index. $L^{\star}$ is indicated by a dotted line on the left-hand figure. The results of a two-sided K–S test for each distribution are presented in Table 2.

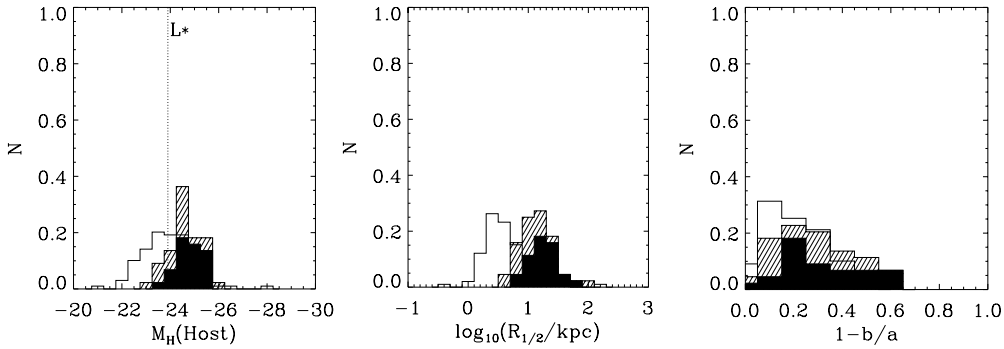

Figure 5. Histograms for the present 3CR sample (open) and the Taylor et al. (1996) quasar sample (full sample—shaded; RLQs—black) for the following properties (from left to right): host galaxy luminosity (converted *H* band); scale length; ellipticity. $L^{\star}$ is indicated by a dotted line on the left-hand figure. The results of a two-sided K–S test for each distribution are presented in Table 2. The Taylor et al. sample is the same as the Dunlop et al. one, but studied at *K* band from the ground (see the text).

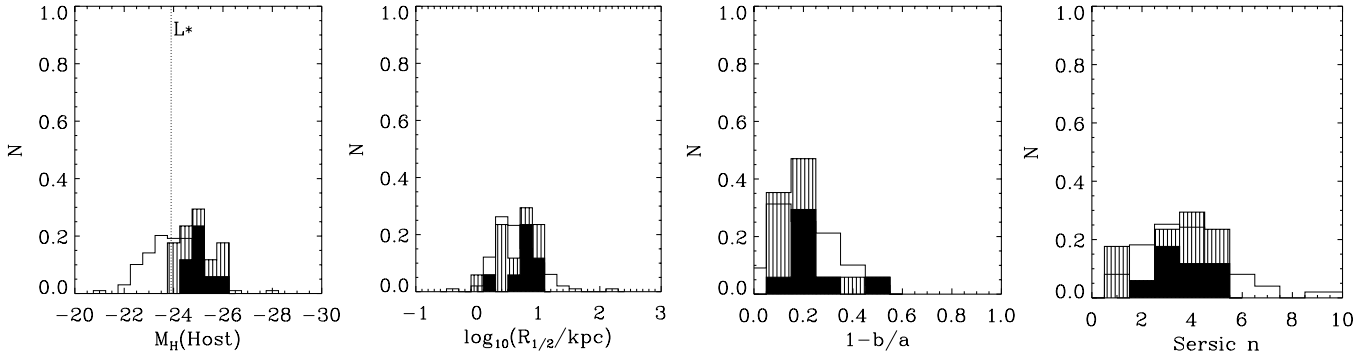

Figure 6. Histograms for the present 3CR sample (open) and the Floyd et al. (2004) quasar sample (full sample—shaded; RLQs—black) for the following properties (from left to right): host galaxy luminosity (converted *H* band); scale length; ellipticity; Sérsic index. $L^{\star}$ is indicated by a dotted line on the left-hand figure. The results of a two-sided K–S test for each distribution are presented in Table 2.

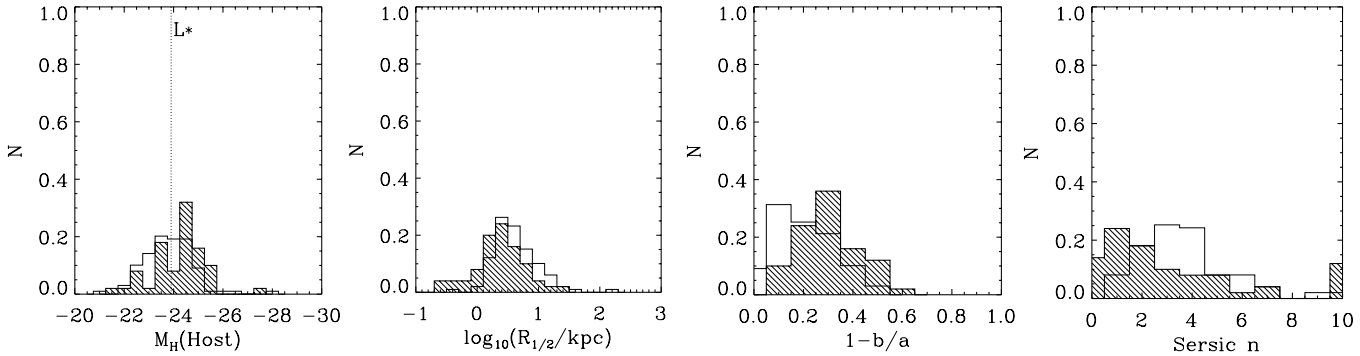

Figure 7. Histograms for the present 3CR sample (open) and the Rothberg & Joseph (2004) merger sample (shaded) for the following properties (from left to right): host galaxy luminosity (converted *H* band); scale length; ellipticity; Sérsic index. $L^{\star}$ is indicated by a dotted line on the left-hand figure. The results of a two-sided K–S test for each distribution are presented in Table 2.

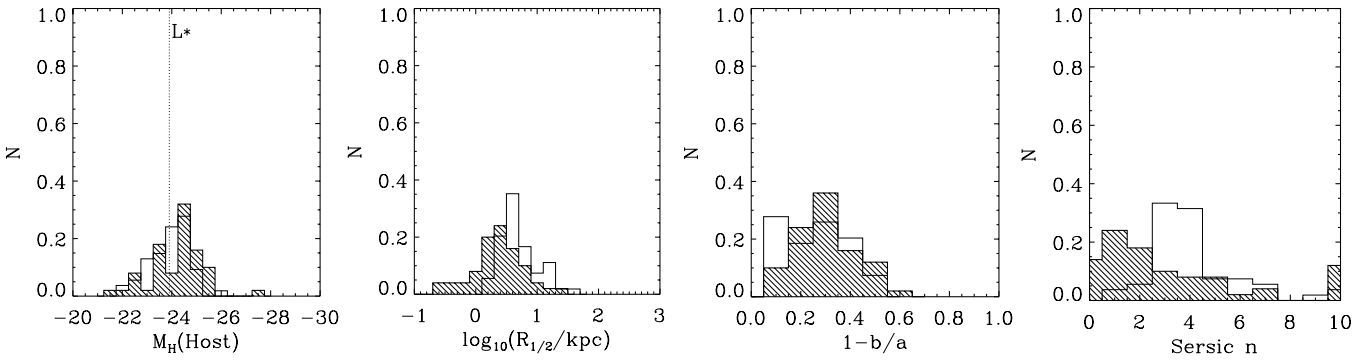

Figure 8. As for Figure 7, but for Rothberg & Joseph (2004, shaded) compared to only those 3CR sources that are flagged as *merger remnants* (open).

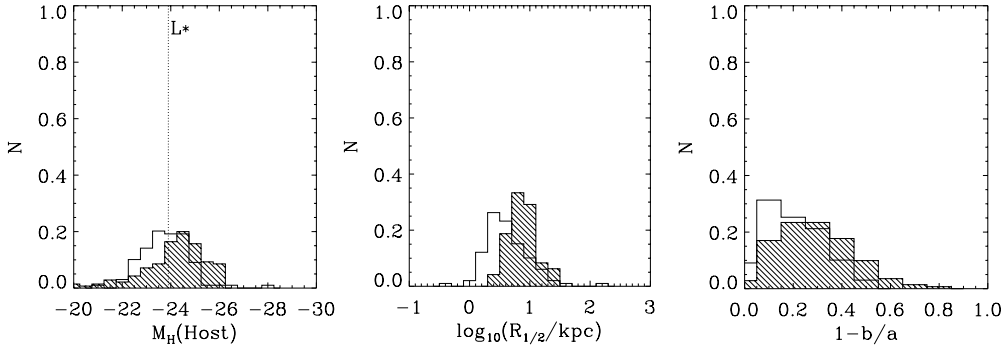

Figure 9. Histograms for the present 3CR sample (open) and Bender et al. (1992) early-type galaxy sample (shaded) for the following properties (from left to right): host galaxy luminosity (converted *H* band); scale length; ellipticity. $L^\star$ is indicated by a dotted line on the left-hand figure. The results of a two-sided K–S test for each distribution are presented in Table 2.

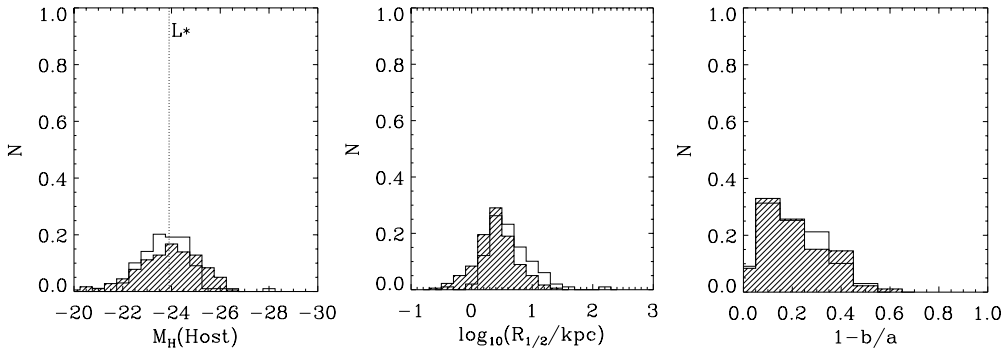

Figure 10. Histograms for the present 3CR sample (open) and the Pahre (1999) early-type galaxy sample (shaded) for the following properties (from left to right): host galaxy luminosity (converted *H* band); scale length; ellipticity. $L^\star$ is indicated by a dotted line on the left-hand figure. The results of a two-sided K–S test for each distribution are presented in Table 2.

ellipticals ($-20.5 \leqslant M_B \leqslant -18.5$), 12 bright dwarf ellipticals ($M_B > -18.5$) as well as 4 compact ellipticals, 19 bulges and 5 lower luminosity dwarf spheroids. Observations and modeling were presented by Bender & Moellenhoff (1987). Observations were made using the Calar-Alto 1.23 m telescope and a NEC P8603/A detector. Modeling followed a similar method to our "one-dimensional" fits to elliptical isophotal values, presented in Paper II. The sample is compared with the 3CR in Figure 9. We adopt this sample as a useful cross section of the elliptical population.

Pahre (1999). Pahre (1999) observed 341 nearby ($z \lesssim 0.03$) early-type galaxies in *K* band using the Palomar 60 inch and the Las Campanas 1 m (Swope) and 2.5 m (Du Pont) telescopes and Rockwell NICMOS3 HgCdTe detectors. Most are from 13 rich clusters (85%), but also with 12% from loose groups and 3% from the general field. These span the full range of early types, forming a useful reference for the 3CR. Modeling was performed in a similar way to our "one-dimensional" fits to elliptical isophotes, as described in Paper II, although all masking was performed automatically, instead of some removal by hand of obvious companion sources as in our modeling. No Sérsic fit is given. Figure 10 illustrates the various properties of the sample compared with those of the 3CR.

Mobasher et al. (1999). Mobasher et al. (1999) studied the Fundamental Plane in a sample of 48 elliptical galaxies (no lenticulars) from the Coma cluster ($\bar{D} = 99$ Mpc) in *K* band. They were selected to have optical half-light diameters of less than 1 arcmin in order to fit into the field of view of IRCAM3 on UKIRT. Curves of growth were produced for each target, rather than a functional form being fitted. Effective diameter and effective mean surface brightness were calculated directly from the curve of growth. Figure 11 illustrates the various properties of the sample compared with those of the 3CR.

Ferrarese et al. (2006). As part of the Advanced Camera for Surveys (ACS) Virgo Cluster Survey, Ferrarese et al. (2006) studied a sample of 100 early-type members of the Virgo cluster

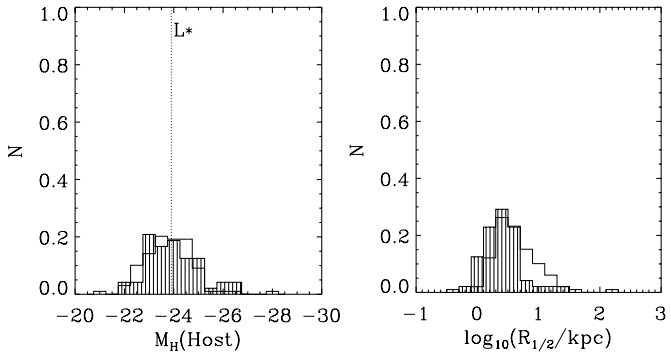

Figure 11. Histograms for the present 3CR sample (open) and the Mobasher et al. (1999) early-type galaxy sample (shaded) for the following properties (from left to right): host galaxy luminosity (converted H band); scale length. $L^{\star}$ is indicated by a dotted line on the left-hand figure. The results of a two-sided K–S test for each distribution are presented in Table 2.

($\bar{D}$ = 18 Mpc) from dwarfs ($M_B = -15.1$ mag) to giants ($M_B = -21.8$ mag) imaged in F475W and F850LP (g and z bands). This forms a useful local early-type galaxy baseline with which to compare our the luminosity of our sample, allowing us to rank the host galaxies of the 3CR against the entire contents of a nearby cluster. Modeling performed by Ferrarese et al. was identical to our ellipse fitting followed by radial profile fits to the elliptical isophote values in Paper II, although Ferrarese et al. also fit core-Sérsic (Graham et al. 2003) models to objects that are sufficiently close to detect a "Nuker"-like (Lauer et al. 1995) turnover or "core" in some of the galaxy centers. We compare results to their z-band data, converted to H as described above. Figure 12 illustrates the various properties of the sample compared with those of the 3CR. We note that many of these objects have noticeable disks in addition to their bulges (S0 types), reflected in their intermediate Sérsic index values. This use of a single Sérsic profile in such cases is questionable.

2.2.4. BCGs

Graham et al. (1996). Graham et al. (1996) took the sample of 119 Abell BCGs ($0.01 < z < 0.054$) originally observed in Cousins R band by Postman & Lauer (1995) on the CTIO 1.5 m and the KPNO 2.1 m and 4 m telescopes. Sérsic profiles were fit to the semi-major axis surface brightness profiles of Postman & Lauer (1995), similar to our "one-dimensional" fitting of profiles to the elliptical isophotal levels in Paper II. Figure 13 illustrates the various properties of the sample compared with those of the 3CR. This remains a state-of-the-art data set for the study of BCGs in spite of the age of the observations.

3. RESULTS

For the full tabulated results of the morphological modeling of each individual source, see Tables 4 and 5 of Paper II. Here, we only discuss those results in a sample-wide comparison. Histograms comparing the distributions of various properties of these samples with those of our 3CR sample are presented in Figures 2–13. We performed a K–S test to compare each property of each comparison sample to the equivalent property of our 3CR sample. This returns the K–S statistic, D, reflecting the cumulative difference between two samples, and a likelihood, p that the two samples are drawn from the same population. Results of the K–S test, showing the goodness of fit between each sample and the 3CR are presented in Table 2. Table 3 shows each sample compared to just the FR I sources in our 3CR sample. Table 4 shows each sample compared to just the FR II sources in our 3CR sample. In the following, we present a broad sample-by-sample comparison, followed by more detailed comparisons in each observational metric (morphology, ellipticity, luminosity, scale length, and the R_e–μ_e Kormendy relation). In the discussion, Section 4, below, we engage in a more detailed discussion of each property.

3.1. Sample-by-sample Comparisons

The BL Lac object host galaxies of the Urry et al. (2000) sample span the upper luminosity and scale length range of the 3CR host galaxies—Figure 2. Galaxies as dim (small) as the very bottom end of the 3CR galaxy luminosity (scale length) distribution are conspicuously missing, and this is also found with the other active galaxy samples discussed below. We return to discuss this point in some detail in Sections 4.2 and 5. Interestingly, the BL Lac object ellipticities overlap nicely with the round majority of the 3CR, but lack the eccentric tail representing merging sources among the radio galaxies. Overall, the BL Lac objects represent a poor fit to the 3CR sample. Even considering the FR I and FR II subsamples separately produces little improvement in the match.

The McLeod & McLeod (2001) RQQ host galaxy luminosities and ellipticities exhibit a good match with the 3CR—Figure 3. The quasar host galaxies appear to be somewhat smaller on average, in contrast to the other samples of quasars discussed below that include both radio-loud and radio-quiet sources. Redshifts range from 0.15 to 0.4 with an average at $\bar{z} = 0.25$.

The Dunlop et al. (2003) quasar host galaxies appear to be consistent with the bright end of the 3CR host galaxy distribution, assuming a simple conversion from R band to

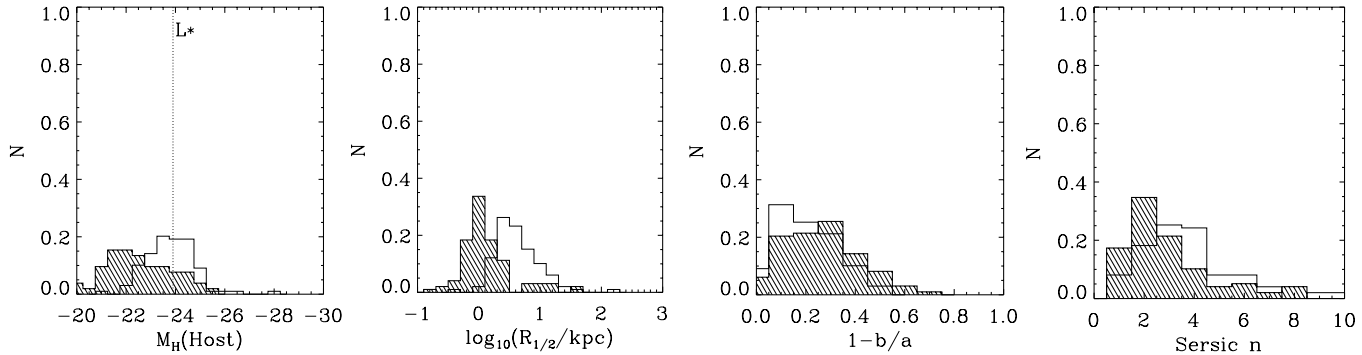

Figure 12. Histograms for the present 3CR sample (open) and the Ferrarese et al. (2006) galaxy Virgo cluster galaxy sample (shaded) for the following properties (from left to right): host galaxy luminosity (converted H band); scale length; ellipticity; Sérsic index. $L^{\star}$ is indicated by a dotted line on the left-hand figure. The results of a two-sided K–S test for each distribution are presented in Table 2.

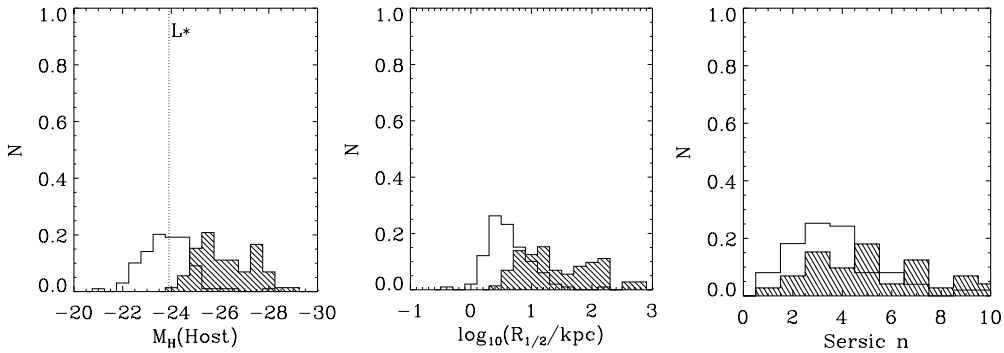

Figure 13. Histograms for the present 3CR sample (open) and the Graham et al. (1996) BCG sample (shaded) for the following properties (from left to right): host galaxy luminosity (converted *H* band); scale length; Sérsic index. $L^{\star}$ is indicated by a dotted line on the left-hand figure. The results of a two-sided K–S test for each distribution are presented in Table 2.

Table 2
Full Sample Statistics: *D* and *p* from the two-sided Kolmogorov Test Comparing the Full 3CR Sample with Each Other Sample

Property	U+00[a]	MM01[b]	D+03[c]	F+04[d]	T+96[e]	RJ04[f]	BBF92[g]	P99[h]	M+99[i]	F+06[j]	G+96[k]
M_H(Host)	0.47	0.34	0.62	0.57	0.44	0.29	0.23	0.15	0.11	0.68	0.81
	0.00	0.06	0.00	0.00	0.00	0.01	0.00	0.11	0.82	0.00	0.00
$R_{1/2}$	0.33	0.32	0.52	0.19	0.62	0.30	0.49	0.26	0.32	0.65	0.60
	0.00	0.09	0.00	0.65	0.00	0.00	0.00	0.00	0.00	0.00	0.00
$\epsilon = 1 - b/a$	0.36	0.15	0.14	0.22	0.26	0.34	0.25	0.06	...	0.20	...
	0.00	0.89	0.67	0.42	0.03	0.00	0.00	0.99	...	0.04	...
n	0.27	...	0.42	0.17	...	0.34	...	...	...	0.29	0.57
	0.12	...	0.00	0.73	...	0.00	...	...	...	0.00	0.00
d	...	...	...	...	...	0.42	0.28	...	...	...	...
	...	...	...	...	...	0.00	0.00	...	...	...	...

References.
[a] Urry et al. 2000.
[b] McLeod & McLeod 2001.
[c] Dunlop et al. 2003.
[d] Floyd et al. 2004.
[e] Taylor et al. 1996.
[f] Rothberg & Joseph 2004.
[g] Bender et al. 1992.
[h] Pahre 1999.
[i] Mobasher et al. 1999.
[j] Ferrarese et al. 2006.
[k] Graham et al. 1996.

H band—see Figure 4. The more certain conversion from *K* (Taylor et al. 1996) to *H* provides a similar picture (Figure 5) though based on less certain host galaxy luminosities due to the less stable ground-based PSF. The higher ellipticities and scale lengths in the Dunlop/Taylor quasars are again possibly due to PSF correction problems. Note that the Dunlop et al. sample exhibits a strong cutoff in Sérsic index in their radio-loud subsample that is *not* mirrored in the 3CR population.

The quasar host galaxy sample of Floyd et al. (2004) again matches the upper reaches of the 3CR host galaxy luminosity distribution, while the scale length, ellipticity, and Sérsic indices all show a similar spread in values—Figure 6. Note that a key finding of both Floyd et al. and Dunlop et al. was the relative similarity of RLQ and RQQ properties, although the smallest and dimmest of the quasar host galaxies in each sample are radio quiet in each case. This is reflected in the histograms presented in Figures 4 and 6.

In general, and unsurprisingly, the Rothberg & Joseph (2004) sample forms a poor match to the 3CR host galaxies (Figure 7). However, if we examine only the subset of 3CR host galaxies that are classed as exhibiting merger signatures (as defined in Paper II), we see some improvement (Figure 8). In particular, there is a noticeable increase in the likelihood that the two samples are drawn from the same ellipticity distribution. But even among these merging 3CR sources, the host galaxies are significantly less disky than the general merger population explored by Rothberg & Joseph and the disk-merger population contains many sources much smaller than the 3CR mergers, while the luminosity distributions span a similar range.

The Bender et al. (1992) sample forms a poor match to the 3CR host galaxies in all observational metrics (see Figure 9), being generally larger and more luminous, as well as slightly more eccentric in shape.

Generally, the Pahre (1999) sample forms a good match to the 3CR host galaxies, although the Pahre sample does exhibit a long low-luminosity/compact galaxy wing, beyond the cutoff in the 3CR host luminosity and scale length distributions—Figure 10. In terms of ellipticity, the match is excellent.

The Mobasher et al. (1999) sample forms a very good match in terms of host galaxy luminosity to the 3CR—Figure 11. It is noticeable that the 3CR galaxies tend to be slightly larger, with a poorer match between the scale length distributions,

Table 3
FR I Statistics: D and p of the two-sided Kolmogorov Test Comparing the 3CR FR I Sample with Each Other Sample

Property	U+00[a]	MM01[b]	D+03[c]	F+04[d]	T+96[e]	RJ04[f]	BBF92[g]	P99[h]	M+99[i]	F+06[j]	G+96[k]
M_H(Host)	0.66	0.55	0.82	0.75	0.62	0.47	0.42	0.30	0.12	0.68	0.87
	0.00	0.00	0.00	0.00	0.00	0.00	0.00	0.03	0.83	0.00	0.00
$R_{1/2}$	0.52	0.13	0.68	0.34	0.76	0.18	0.67	0.13	0.14	0.50	0.73
	0.00	0.99	0.00	0.15	0.00	0.58	0.00	0.80	0.86	0.00	0.00
$\epsilon = 1 - b/a$	0.33	0.22	0.22	0.23	0.38	0.46	0.37	0.18	...	0.34	...
	0.05	0.69	0.44	0.58	0.01	0.00	0.00	0.41	...	0.01	...
n	0.42	...	0.57	0.34	...	0.36	...	...	...	0.10	0.70
	0.02	...	0.00	0.14	...	0.02	...	...	...	0.99	0.00
d	...	...	...	...	...	0.46	0.30	...	...	...	...
	...	...	...	...	...	0.00	0.03	...	...	...	...

References.
[a] Urry et al. 2000.
[b] McLeod & McLeod 2001.
[c] Dunlop et al. 2003.
[d] Floyd et al. 2004.
[e] Taylor et al. 1996.
[f] Rothberg & Joseph 2004.
[g] Bender et al. 1992.
[h] Pahre 1999.
[i] Mobasher et al. 1999.
[j] Ferrarese et al. 2006.
[k] Graham et al. 1996.

Table 4
FR II Statistics: D and p of the two-sided Kolmogorov Test Comparing the 3CR FR II Sample with Each Other Sample

Property	U+00[a]	MM01[b]	D+03[c]	F+04[d]	T+96[e]	RJ04[f]	BBF92[g]	P99[h]	M+99[i]	F+06[j]	G+96[k]
M_H(Host)	0.47	0.29	0.61	0.54	0.43	0.25	0.23	0.15	0.28	0.74	0.82
	0.00	0.20	0.00	0.00	0.00	0.06	0.03	0.26	0.11	0.00	0.00
$R_{1/2}$	0.28	0.40	0.48	0.18	0.64	0.37	0.46	0.30	0.37	0.74	0.62
	0.03	0.03	0.00	0.78	0.00	0.00	0.00	0.00	0.00	0.00	0.00
$\epsilon = 1 - b/a$	0.39	0.14	0.17	0.26	0.20	0.29	0.20	0.10	...	0.15	...
	0.00	0.95	0.55	0.30	0.23	0.02	0.07	0.77	...	0.40	...
n	0.28	...	0.41	0.20	...	0.43	...	...	...	0.41	0.60
	0.14	...	0.00	0.63	...	0.00	...	...	...	0.00	0.00
d	...	...	...	...	...	0.41	0.28	...	...	...	...
	...	...	...	...	...	0.00	0.00	...	...	...	...

References.
[a] Urry et al. 2000.
[b] McLeod & McLeod 2001.
[c] Dunlop et al. 2003.
[d] Floyd et al. 2004.
[e] Taylor et al. 1996.
[f] Rothberg & Joseph 2004.
[g] Bender et al. 1992.
[h] Pahre 1999.
[i] Mobasher et al. 1999.
[j] Ferrarese et al. 2006.
[k] Graham et al. 1996.

due to the field-of-view imposed size cutoff in the Mobasher sample.

Unsurprisingly, the 3CR host galaxies are much larger and more luminous than the typical cluster galaxy represented by the Ferrarese et al. (2006) sample—Figure 12. However, they also exhibit larger Sérsic indices in general, in spite of the fact that Ferrarese et al. deliberately study only morphologically selected early-type galaxies. Many of the Ferrarese objects are S0's with noticeable disks in addition to their bulges, yielding intermediate Sérsic values. S0's are not accurately represented with a single Sérsic profile.

The 3CR host galaxies span a far lower range of luminosity than the BCGs of Graham et al. (1996), are significantly smaller and have lower Sérsic indices—Figure 13. The distributions have dissimilar shapes but there is significant overlap in terms of Sérsic index.

3.2. Host Galaxy Morphology

We find a broad distribution of Sérsic indices in our sample, spanning the full range from $n = 1$ (exponential disks) to

$n = 4$ (de Vaucouleurs ellipticals), and higher. In Paper II, we discussed the FR II radio sources that are hosted by disk-like ($n < 2$) galaxies, all of which have close companion objects and are either merging, or are likely to be post-merger systems. In comparison with normal cluster early types (Figures 9—12), this range of Sérsic index is not unusual. For example, by comparison to the local sample of Ferrarese et al. (2006), the *range* of Sérsic index is identical, but the peak in Sérsic index in our sample falls significantly higher: in the Virgo cluster, the peak Sérsic index is at $n = 2$, with a significant lower-n tail, whereas in the 3CR, the peak is at $n = 3$, and the tail exhibits a much more rapid falloff to low-n (Figure 12). When we compare the Ferrarese sample to only the FR I's in the 3CR there is a dramatic improvement ($D = 0.10$; $p = 0.99$), with both populations exhibiting similar peaks in the Sérsic index distribution. However, whereas the Ferrarese objects are typically S0's with distinct bulge and disk components, the FR I's are typically found in diffuse giant (D, cD) elliptical galaxies (Owen & Laing 1989). Both populations are better described using two Sérsic profiles.

In comparison with the BCGs of Graham et al. (1996), there is again a clear distinction with the BCGs exhibiting a far larger range of n to high values (Figure 13). The peak in the BCG Sérsic index distribution is close to $n = 5$, with a number of objects having $n > 10$. However, at the low-n end, the 3CR closely follows the cutoff in Sérsic index seen in these most massive cluster-dominating galaxies. These sources are also be better fit by a two-Sérsic component model (Seigar et al. 2007).

Morphology also distinguishes the 3CR host galaxies from typical merger systems that have Sérsic indices even lower than the cluster ellipticals, peaking at $n = 1$ (Figure 7). These sources are posited as post-merger systems on their way to forming massive ellipticals, but not generally the first-ranked elliptical galaxies in clusters (Rothberg & Joseph 2004; Rothberg & Fischer 2010). Even when comparing to only the 3CR sources flagged as mergers in Paper II, we see a far stronger tendency for the 3CR mergers to be identified as bulge dominated ($n > 2$) than the general merger population (Figure 8).

The morphologies of the sample do fit in well with the (far smaller) QSO samples of Dunlop et al. (2003) and Floyd et al. (2004)—see Figures 4 and 6. However, these QSO hosts appear to show a bimodal distribution, with a smaller disky ($n = 1$) peak, as well as the elliptical peak close to $n = 4$. As noted by Floyd et al. (2004), however, the three disky objects are all RQQ's, at low-optical luminosity similar to a classical Seyfert galaxy. The same is true for the Dunlop sample. Thus, while the 3CR are morphologically similar to the RLQs studied in each of these papers, they are distinct from the general host galaxy population of RQQ's. Using our own Sérsic fits to the Urry et al. (2000) BL Lac object sample, we find a similar spread in Sérsic indices, although there is a long tail to high values among the BL Lac objects.

3.3. Ellipticity

The ellipticity distribution of the 3CR matches very well with that of the Pahre (1999) sample of K-band studied elliptical galaxies drawn from a range of environments (K–S test: $D = 0.06$; $p = 0.99$). However, the samples of Bender et al. (1992); Ferrarese et al. (2006), which focus on entire populations from a cluster, show (typically E2–E3) ellipticity distributions that are closer to that of the mergers than that of the 3CR. Disney et al. (1984) also found that radio-loud ellipticals are inherently rounder than radio-quiet ones. Unfortunately, no ellipticity data is available for the BCGs, but they are quite round in general (from visual inspection of the original data of Postman & Lauer 1995).

The quasar data seems to support a similar ellipticity distribution for both the Floyd and the Dunlop samples ($D = 0.22$; $p = 0.42$ and $D = 0.14$; $p = 0.67$, respectively). In particular, the radio-loud objects exhibit similar peaks at around E1 in both samples, but there is an additional highly elliptical (E5) peak in both quasar samples that may be due to small number statistics, or indicate objects in which asymmetries from the PSF have interfered with proper characterization of the quasar host galaxy.

The most striking contrast in terms of ellipticity is with the merger remnants of Rothberg & Joseph (2004)—see Figure 7 ($D = 0.34$; $p = 0.001$). The merger remnants typically have much higher median ellipticities (E3) than those of the present 3CR sample (E1). This is perhaps unsurprising given that the Rothberg & Joseph sample is targeted at objects that have recently undergone a major merger and have not had time to fully relax to their (presumably elliptical galaxy) endpoints. But it does demonstrate quite graphically that the powerful radio sources are not, in general, consistent with recent major-merger systems. However, if we turn our attention to those objects in the 3CR that exhibit any kind of tidal or merger-like disturbances (flagged with mergers, shells, or tidal tails in Paper II), we find a somewhat different situation—see Figure 8: a bimodal ellipticity distribution that follows the ellipticity distribution of Rothberg & Joseph's mergers somewhat better ($D = 0.20$; $p = 0.22$).

3.4. Galaxy Luminosity

The low-z 3CR host galaxy population peaks at close to $L^\star$ ($M_H = -23.9$), but with significant spread. The high end is dominated by the FR II sources, but there are several FR II sources in the low-luminosity wing as well. The merger systems studied by Rothberg & Joseph are generally as luminous as the 3CR host galaxies, if not more so. Rothberg & Joseph conclude that these systems end up largely as $L^\star$ (or brighter) elliptical galaxies after the starburst fades.

Comparing with elliptical galaxies in general, we see a good match in host luminosity distribution with the sample of Mobasher et al. (1999; $D = 0.11$, $p = 0.82$)—particularly to the FR I's ($D = 0.12$; $p = 0.83$). The sample of Pahre (1999) gives a somewhat poorer match ($D = 0.15$; $p = 0.11$) which is improved if we look only at the FR II's ($D = 0.15$; $p = 0.26$). The Ferrarese et al. (2006) sample covers the entire Virgo cluster, and understandably peaks at far lower luminosities, but it is instructive to see the crossover between the 3CR and the entire contents of such a cluster (Figure 12). The 3CR hosts are representative of the top one third, in terms of luminosity, of the galaxies in Virgo. While there is some overlap with the BCG population, in general, when compared, the 3CR's are smaller and less luminous. While the FR I's were found to have a similar Sérsic index distribution, any apparent similarity with the Ferrarese sample is eliminated by comparing their luminosities.

The median luminosity of the 3CR host galaxies is somewhat dimmer than that of the typical quasar host galaxy, or BL Lac object, based on simple transformations from the fluxes of Urry et al. (2000); Dunlop et al. (2003) and Floyd et al. (2004) assuming an old stellar population (see Section 2.1). We acknowledge that there are difficulties in comparing to

luminosities measured in different bands in this manner, but with the existing samples of low-redshift quasar host galaxies, a single band is generally all that can be compared, and so there is no constraint on the mass-to-light ratios of these objects. However, for the Dunlop et al. sample, ground-based *K*-band imaging was published in an earlier paper by Taylor et al. (1996), offering us a convenient test-case: although the *K*-band morphologies are less reliable due to the problem of disentangling the host and the nucleus from the ground, luminosity in most cases is well constrained, and they can be much more reliably converted into an *H*-band luminosity. We see an essentially identical luminosity distribution to that exhibited by the Dunlop/Taylor data—Figures 4 and 5. Once again, we see a significant population of sub-$L^\star$ 3CR hosts that are not mirrored in the quasar population. As was stated earlier and in Paper II, the low-luminosity 3CR objects tend to be low-redshift, low-radio-power FR I sources. We note that the Urry et al. (2000) sample exhibits a slightly greater crossover in luminosity with the 3CR at this low end, in accord with the unification of these objects with the BL Lac objects, but there remains a deficit of the faintest objects seen in the 3CR.

3.5. Galaxy Scale Length

The 3CR host galaxy scale lengths, in keeping with the host galaxy luminosities, are typical of large ($\sim L^\star$) elliptical galaxies, with a median of 3.6 kpc, and a few sources larger than 10 kpc in size. They are somewhat smaller than reported in many parts of the quasar literature, but are consistent with those of Floyd et al. (2004; $D = 0.19$, with $p = 0.65$) and somewhat consistent with McLeod & McLeod (2001; $D = 0.32$, with $p = 0.09$). They are inconsistent with the scale length distributions reported by Urry et al. (2000; $D = 0.33$, $p = 0.002$), Dunlop et al. (2003; $D = 0.52$, $p \sim 10^{-4}$), and Taylor et al. (1996; $D = 0.63$, $p \sim 10^{-9}$). The latter data set in particular is known to overestimate the scale lengths, due to atmospheric seeing problems: compare results with Dunlop et al. (2003), who study the same sample in *R* band using *HST* data—Figures 4 and 5. The Taylor et al. ground-based work generally recovers accurate host galaxy luminosities (see Dunlop et al. 2003), but poorly constrained morphological parameters, such as scale length and surface brightness. That the 3CR scale lengths agree at least with the Floyd et al. quasar sample is reassuring, and it is possible that earlier studies overestimated the quasar host galaxy scale lengths somewhat. Considering the 3CR FR II sources alone, we get a considerable improvement to the comparison with the Floyd et al. quasars ($D = 0.18$; $p = 0.78$). Considering 3CR FR I sources alone, we find a significant improvement in the comparison to the McLeod & McLeod (2001) RQQ host galaxy scale lengths ($D = 0.13$, with $p = 0.99$).

While the Merger sample of Rothberg & Joseph (2004) is generally as luminous as the 3CR, we find that in general, the 3CR host galaxies are somewhat larger, consistent with the merger's fluxes being dominated by active star formation in their inner regions.

Comparing to normal elliptical galaxies, there are no statistically good matches in terms of scale length. The 3CR are slightly larger, on average, than the Pahre sample and Mobasher et al. sample of ellipticals, but smaller than the BBF92 sample. Interestingly, the 3CR span the noticeable gap in the Ferrarese sample scale length distribution (Figure 12). The 3CR are smaller, in general, than the Graham et al. BCGs which lack objects smaller than 2 kpc.

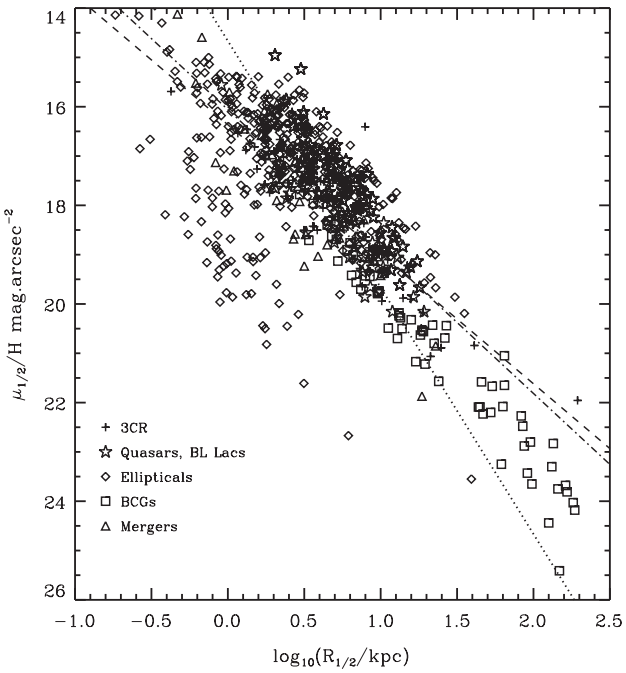

Figure 14. Scale length–surface brightness for the 3CR along with comparison samples (after conversion to *H* band) of quasar and BL Lac object host galaxies, quiescent ellipticals, BCGs and mergers as presented in the text. Best-fitting scale length–surface brightness relations are shown for the FR I's (dashed) and the FR II's (dot-dashed). The locus of an $L^\star$ galaxy is shown by the dotted line. The 3CR fits in well with the structural properties of the giant ellipticals, and is distinct from the dwarf elliptical subsample within the Ferrarese et al. (2006) sample from the Virgo cluster.

3.6. Kormendy Relation (R_e–μ_e)

The strong correlation between scale length and surface brightness is a well-known feature of bright elliptical galaxies (Kormendy 1977), and is a projection of the more physically significant "fundamental plane." The relation followed by the present low-redshift 3CR sample is close to that of quiescent massive elliptical galaxies, following a slope of 2.97 ± 0.1 (Paper II). The BCGs follow a similar trend but extend to far larger radii. The same relation is also a good fit to the quasar host galaxy data of Dunlop et al. (2003) and Floyd et al. (2004). This provides strong evidence that all of these objects are structurally similar, dynamically relaxed systems, although proof of this requires spectroscopy to study the dynamics. Mergers too fit remarkably well with the overall trend in the AGN and quiescent elliptical populations. Putting all of the samples together, including the Virgo cluster galaxies of Ferrarese et al. (2006) results in the plot shown in Figure 14. It is clear here that the giant ellipticals, and powerful AGN (quasars, radio galaxies, and BL Lac objects) form a single population in the R_e–μ_e space. Dwarf ellipticals do not obey the same trend (Capaccioli & Caon 1991; Graham & Guzmán 2003): for a given scale length, these objects are far dimmer than their cousins on the Kormendy relation, and these objects are clearly not represented by the 3CR. The Rothberg & Joseph (2004) mergers appear to be on the low side of the typical elliptical galaxy Kormendy relation.

4. DISCUSSION

4.1. Host Galaxy Morphology

The modeling used in this paper is deliberately simple, aimed at fitting the bulk of each galaxies flux with the minimum of

parameters. Many, if not all, luminous galaxies have core regions that deviate from simple Sérsic models, and which may be detected in many of the closest objects presented here, but in the interests of comparing like with like we have adopted a Sérsic model and compared to the large literature on fitting similar models to control samples of galaxies and quasars. Regarding morphology of quasar host galaxies, it is difficult to distinguish an $n = 6$ bulge, say, from an $n = 4$ one underneath the glare of a quasar nucleus ($M_V \leqslant -23$). The spread in n present in the 3CR host galaxies does in fact connect them more firmly with the quiescent elliptical galaxy population, which does not in general follow a perfect de Vaucouleurs type $r^{1/4}$ law which tends to be seen in quasar host galaxies. It seems likely that when applying such morphological models to the host galaxies of quasars, there is insufficient signal under the photon shot noise in the central region to accurately determine n in many cases: although it is clear that in most cases the difference between an elliptical or bulge-dominated and disky or disk-dominated host is measurable (McLure et al. 1999; McLeod & McLeod 2001; Dunlop et al. 2003; Floyd et al. 2004), it is difficult to determine the precise morphology as characterized by a single continuous parameter given current observational technology.

The 3CR host galaxies follow the same Kormendy relation to the host galaxies of quasars and giant ellipticals (Figure 14): even the very lowest luminosity ones are clearly distinguished from the dwarf ellipticals. However, what is clearly missing is dynamical information on these sources that would provide a real physical insight into the conditions inside the host galaxies. A study of southern radio galaxies by Bettoni et al. (2001) has shown that those sources are indeed hosted by dynamically relaxed elliptical galaxies. The closest comparison sample is that of Mobasher et al. (1999) which already has suitable spectroscopic data. It would be a valuable study to investigate the relative dynamical states of these two samples. Spectroscopic data for the 3CR host galaxies would enable us to determine the dynamics and stellar populations of these objects in order to explore their ages, merger histories, and the differences between sources lying in rich environments and those lying in the field.

4.2. Host Galaxy Luminosity

The most surprising finding from this survey has been the relative faintness in H band of a small number of the 3CR host galaxies relative to the luminosities expected from studies of quasar host galaxies. Even when we consider only FR II sources, several host galaxies exist that are rather fainter than the cutoff of $\sim L^\star$ inferred from the RLQ host galaxy luminosity functions of Dunlop et al. (2003) and Floyd et al. (2004). Assuming a mass-to-light ratio for early-type galaxies in general, $M/L_H \sim 1.2$ (with a scatter of 0.2 dex; Zibetti et al. 2002), we have just three sources with masses $> 5 \times 10^{11}\ M_\odot$: 3C 130, 3C 196.1, and 3C 338. Firstly, we note that the median mass of the sample estimated in this simplistic way is $10^{11}\ M_\odot$ and the mean mass $2 \times 10^{11}\ M_\odot$. This is significantly higher than the $\sim 3 \times 10^{10}\ M_\odot$ mass cutoff inferred for a transition in galaxy formation mode (Kauffmann et al. 2003; Khochfar & Silk 2006, 2009). Secondly, the vast majority of the anomalously faint tail ($M_H > -23$) in the 3CR host galaxy distribution is made up of very nearby (11 at $z < 0.05$, 19 at $z < 0.1$) radio sources that are relatively radio-dim, some even classically "radio quiet" by the simplistic standard adopted for the RLQ/RQQ break in quasar studies. These sources would not be selected as part of the 3CR if they lay just a little more distant and cannot properly be compared with RLQs. Just two of the sources with faint host galaxies, 3C 61.1 (an FR II) and 3C 314.1 (an FR I), lie at higher redshifts ($z = 0.186$ and $z = 0.119$, respectively). In addition, seven of the lower redshift sources are worth considering: 3C 105, 3C 198, 3C 227, 3C 326, 3C 353, 3C 402, and 3C 445 are all FR II radio sources in abnormally dim galaxies. These objects are discussed in greater detail in the following section. Finally, we remark that just two of these dim FR II host galaxies (3C 61.1 and 3C 445) have simple estimated masses below the $\sim 3 \times 10^{10}\ M_\odot$ mass cutoff inferred for a transition in galaxy formation mode (Kauffmann et al. 2003; Khochfar & Silk 2006, 2009).

It is interesting to explore how this finding compares to statistical surveys of nearby radio galaxies. The largest sample is that of Mauch & Sadler (2007) who examined 7824 radio sources from the 1.4 GHz NRAO VLA Sky Survey (NVSS) with galaxies brighter than $K = 12.75$ mag from the 6 degree Field Galaxy Survey (6dFGS). The galaxies in the 6dFGS span the redshift range $0.003 < z < 0.3$, making an ideal comparison to the samples presented here. Typical colors for early-type galaxies are $H - K \approx 0.2$–0.5. Galaxies with luminosities $M_K > -23$ are extremely rare—rarer than we find for $M_H > -23$. However, we note that the 6dFGS cutoff will lose $M_K > -23$ galaxies at $z \approx 0.033$ and even $M_K > -23.5$ galaxies at just $z \approx 0.041$. Thus, it appears that this rare population was essentially invisible to earlier surveys and have only been discovered by virtue of deep imaging of a purely radio-selected sample.

4.3. FR-type and Unification

Fanaroff & Riley (1974) showed that radio galaxies exhibit a change in morphology at a monochromatic power corresponding to roughly $10^{24.5}$ W Hz^{-1} at a rest-frame frequency of 1.4 GHz (converted from the original cutoff at 178 MHz—Bicknell 1995). It is understood that the two classes have different bulk energy transport mechanisms (Bicknell 1995 and references therein). Owen & Ledlow (1994) showed that on the optical–radio plane, the division between the two classes, which occurs over a full decade in radio power, becomes much cleaner. Urry et al. (2000) took this a stage further by looking at just the extended radio power (subtracting off the core from the total) and the optical luminosity of the host galaxy alone. To do this, they used the 5 GHz radio flux which is sensitive to core emission and provides a core/extended distinction for the largest possible sample. This avoids the effects of beaming and cleans up the division between FR I/BL Lac object and FR II/quasar even further. The dividing line was found to follow that predicted by the models of Bicknell (1995), with the FR I sources containing turbulent, transonic jets, and FR II sources jets that are super or hypersonic (see Bicknell 1995 and references therein). This line was later found to be consistent with a constant Eddington accretion ratio (Ghisellini & Celotti 2001). In Figure 15, we plot the available 5 GHz data for the present sample (Jenkins et al. 1977; Giovannini et al. 1988), along with RLQs from Dunlop et al. (2003) and Floyd et al. (2004), and BL Lac objects from Urry et al. (2000). The division confirms once again that FR I's are unified with BL Lac object sources, while FR II's are analogous to RLQs.

We also note that a number of "radio-quiet" quasars studied by Dunlop et al. and Floyd et al. may actually occupy a similar region of the host luminosity–extended radio power plane to the FR I's and BL Lac objects, if their radio luminosities are dominated by an extended component. This is uncertain since RQQs have not been studied in such great depth in the radio as RLQs, and nothing is known of their radio structure.

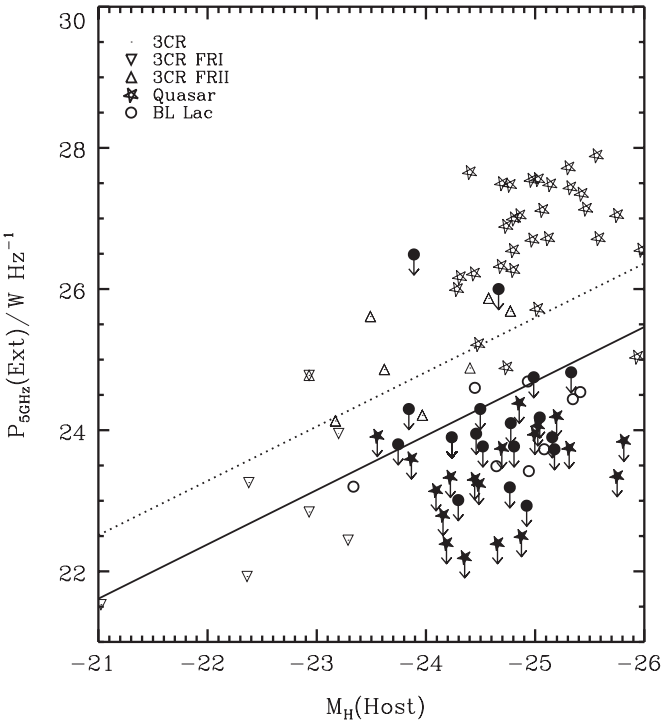

Figure 15. FR-type diagnostic can be made according to optical luminosity vs. radio power, according to Owen & Ledlow (1994). Using only extended radio power and host galaxy luminosity avoids the effects of beaming (Urry et al. 2000). Models from Bicknell (1995) are overplotted (solid line: $\gamma_{\rm max}/\gamma_{\rm min} = 10^4$, $\nu_c = 10^{10}$ Hz, $f = 1$; dotted line: $\gamma_{\rm max}/\gamma_{\rm min} = 10^4$, $\nu_c = 10^{11}$ Hz, $f = 0.5$). For comparison, we have plotted the RQQ's (filled stars) from Dunlop et al. (2003) and Floyd et al. (2004), assuming that all their radio flux is extended. Symbols used are the same as in Figure 1, with filled symbols indicating radio-quiet objects and open symbols radio-loud objects.

5. SOURCES WITH FAINT HOST GALAXIES

In this section, we discuss the eight FR II radio sources with anomalously faint ($M_H > -23$) host galaxies and the unusually radio-powerful FR I, 3C 314.1. Extinction maps were generated for these nine sources by dividing the optical WFPC2 images (de Koff et al. 1996; Martel et al. 1999) by the NICMOS images, after registering, scaling, and smoothing the former to the plate scale and resolution of the latter. In several cases, the optical–IR colors suggest strong extinction, sufficient to close some of the gap to $L^\star$ in H band, but not all of it. Note there are an additional four with intermediate luminosities $-23 < M_H < L^\star$: 3C 111, 3C 234, 3C 371, and 3C 390.3 which we do not discuss here.

3C 61.1. It is an FR II radio source in an under-luminous host galaxy ($M_H = -22.2$), with apparent spiral arm structure (see Paper II and references therein) in spite of its high radio power ($\log_{10} L_{178} = 26.27$). However, this source is the brightest member of a small group of galaxies visible on the NICMOS image, and is probably associated with a larger cluster that includes a radio-quiet AGN at $z = 0.184$ (Kristian et al. 1978) some 30″ to the east. It is clearly very dusty from the optical morphology (de Koff et al. 1996). The extinction map is complicated by the star formation in the apparent spiral arms, but the central region appears to be heavily obscured, and we estimate $\sim 0.5H$ mag of extinction in the central region of this source (assuming a diffuse dust model after Mathis 1990), giving an unextincted H-band luminosity of $M_H = -22.7$. It is likely to be the brightest cluster member (though this is uncertain without a proper study of the host galaxy of the nearby AGN).

3C 105. It is an FR II radio source at $z = 0.089$, hosted by a highly flattened and faintly disturbed (in our H-band image) elliptical with M_H(Host) $= -22.88$. The host galaxy of 3C 105 is known to be exceptionally red, with strong stellar absorption lines (Tadhunter et al. 1993; Cohen et al. 1999), and both existing optical *HST* images provide insufficient detection to produce a color-map. We estimate an $R - H$ color for the host galaxy of $\approx 8 \pm 2$ (very approximate due to the barely 3σ detection in R band) indicating a very heavily obscured host galaxy. Cohen et al. commented that the lack of polarized flux could be due to the obscuration of the scatterers, but discount this hypothesis on the basis that the obscuring material would have to cover a large fraction of the ISM. The *HST* images, although shallow in the optical, suggest that a large quantity of absorbing material could indeed be the cause.

3C 198. It is an FR II radio source at $z = 0.081$ in a slightly elongated elliptical host galaxy with M_H(Host) $= -22.55$ and a detectable nuclear point source. The IR nucleus and lack of common reference points on both the H band and optical images mean that we were unable to produce a reasonable color-map. This source appears to be the brightest member of a small group (see McHardy 1974).

3C 227. It is a broad-line FR II radio galaxy at $z = 0.086$. We can clearly see the host galaxy ($M_H = -22.66$) and the bright active nucleus on this NIR image. Both the optical and UV images show a very bright unresolved nucleus (Martel et al. 1999; Allen et al. 2002). The strength of the nucleus destroys any information on the color-map. However, Cohen et al. (1999) found a strong Balmer decrement, and a likely V-band extinction of $A_V \approx 1.7$ mag. using Keck spectropolarimetry. They and Prieto et al. (1993) conclude that the intrinsic brightness of the object is likely to put it in the quasar class. We would conservatively estimate $A_H \approx 0.3$ based on these earlier findings, assuming a diffuse ISM dust model (Mathis 1990).

3C 314.1. It is an abnormally radio-powerful FR I radio source ($\log_{10} L_{178} = 25.42$) in a faint host galaxy ($M_H = -22.96$). It is apparently not in any cluster (Allington-Smith et al. 1993), exhibiting an under-density of nearby galaxies relative to an average elliptical. It shows no major extinction features in the optical–IR color-map, and is unusually blue for an elliptical galaxy ($R - H \approx 1.5$). We note that this object is flagged by Buttiglione et al. (2009) as a relic radio galaxy which is no longer being actively powered by the jet.

3C 326. It is an FR II radio source and exhibits a LINER spectrum (Simpson et al. 1996), and the host galaxy is quite dim ($M_H = -22.99$) and red ($R - H = 2.4$). From the optical image (de Koff et al. 1996), it is extremely dusty, and appears to be an edge-on S0. The color-map shows up to 0.3 H mag of extinction in the central regions of 3C 326 (assuming a diffuse dust model after Mathis 1990), suggesting an unextincted galaxy luminosity of $M_H \approx -23.3$.

3C 353. It is an FR II radio source with a LINER spectrum (Simpson et al. 1996) hosted by a round giant elliptical with M_H(Host) $= -22.99$ at $z = 0.03$. There are no signs of disturbance, with very circular ($e \approx 0.04$) isophotes on the optical image (Martel et al. 1999). The color-map shows a smooth gradient in extinction, with the highest values up to $V = H = 2.7$ at the center, where a small dust lane is visible near the core (de Koff et al. 2000). We estimate $A_H \approx 0.1$ mag for this source in the central region, assuming a diffuse dust model after Mathis 1990.

3C 402. It is an FR II radio source hosted by a smooth, elongated elliptical galaxy with M_H(Host) $= -22.94$ at

$z = 0.023$. The galaxy is found to be quite red, with $V - H = 3.0$ on average, rising to around 3.5 in the central regions.

3C 445. It is an FR II radio source hosted by a M_H(Host) = −22.21 round elliptical at $z = 0.056$. In both the optical and IR images, the morphology is dominated by the bright nuclear point source. This point source dominates the color-map which thus provides no useful information on extinction. Cohen et al. (1999) deduce between about 1.1 and 2.5 mag of *V*-band extinction from their spectropolarimetric study. This is enough provide up to 0.45 *H* mag of extinction assuming a diffuse dust model after Mathis 1990.

All of the sources discussed above merit closer attention to determine their stellar and black hole masses. We note that all except two (3C 61.1, 3C 445) of these low-mass objects are above the Kauffmann et al. (2003) $3 \times 10^{10}\,M_{\odot}$ cutoff (given our mass-to-light ratio assumptions) but all are significantly less luminous than typical quasar host galaxies. Two of the abnormally faint FR II host galaxies (3C 61.1, 3C 198) are found to be the brightest galaxies in a small cluster or group. The remaining six FR II's show anomalously red colors, but insufficient evidence of extinction to bring them up to $L^{\star}$. The FR I source 3C 314.1 is the only unusually blue galaxy. None of the faint objects correspond to the five disky (low-*n*) FR II galaxies discussed in Paper II and mentioned in Section 4.1. Those objects were all found to have close companions and either to be undergoing merger or to be likely recent post-merger systems.

Other published exceptions to the general rule include PKS 0131–36, 0313–192, and PKS 1413+135. PKS 0131–36 is a nearby FR II radio source hosted by a typical S0 galaxy, NGC 612 (see Emonts et al. 2008 and references therein). 0313–192 is a powerful ($\sim 10^{24} h_{75}^{-2}$W Hz^{-1} at 20 cm) FR I radio source in a highly flattened disk-dominated galaxy (Ledlow et al. 1998, 2001). PKS 1413+135 is a "red quasar" with BL Lac object properties in the NIR, but no noticeable optical nucleus, located in a disky galaxy with large amounts of dust obscuration (Perlman et al. 2002 and references therein).

6. QUASARS AND RADIO GALAXIES IN CONTEXT

It remains curious that the low-luminosity and low-*n* sources do not appear in existing samples of RLQ host galaxies. This may be simply explained through the different methods of selection: in the 3CR, we observe all the brightest radio-objects in the northern sky, and these may be bright due to any combination of intrinsic luminosity, proximity, and beaming. In the RLQ samples of Dunlop et al. (2003) and Floyd et al. (2004), care has been taken to remove artificially "radio-loud" sources by avoiding sources that are likely to be beamed—objects that *would* appear in the 3CR are dropped from the RLQ samples. However, we also note that Best et al. (2005) find no correlation between radio power and black hole mass for radio-loud objects. Thus, it should not necessarily be expected that beamed sources should have fainter host galaxies.

Much of the drive in quasar host galaxy studies has been to confront the technical challenge of observing the host galaxies most luminous quasars. In selecting for optically luminous quasars (radio-loud or radio-quiet), there is a dual selection effect for larger, more luminous host galaxies: a priori we do not know whether the luminosity is host galaxy or AGN-dominated; and if optical quasars push the Eddington limit (Floyd et al. 2004), we are likely select for more massive black holes and thus (through the well-known black hole to bulge mass correlation) more massive host galaxy bulges. Radio selection does not necessarily select for high black hole mass since the radio luminosity is 2–3 orders of magnitude lower than the Eddington limit (Ghisellini & Celotti 2001).

It is possible that samples of RLQs are simply not sufficiently large to have detected such comparatively rare faint objects, of which we only find eight in the present 3CR sample, or that techniques are insufficiently sophisticated to detect them with current technology (i.e., "naked quasars"). Additionally, it is possible that quasar host galaxy luminosities can be overestimated due to scattered light from the nucleus (Young et al. 2009), or due to PSF contamination issues (Kim et al. 2008). We feel that this latter effect is unlikely to be a problem in the Dunlop, Taylor and Floyd samples, given the detailed statistical analysis and testing of the method provided by McLure et al. (1999); Floyd et al. (2004, 2008). Finally, we note that any strong star formation in the quasar host galaxies will have the effect of boosting the optical luminosities relative to the simple model assumed here. This will in effect bring the bulk luminosities of the quasar host galaxies down toward the mean luminosity of our sample.

While there is a noticeable disagreement with the results of quasar host galaxy studies, we find that the 3CR radio galaxies are not unusual with respect to the normal elliptical galaxy population. Indeed, only two FR II sources—3C 61.1 and 3C 445—have galaxies dim enough to fall below $3 \times 10^{10}\,M_{\odot}$ (Kauffmann et al. 2003; Khochfar & Silk 2006, 2009) assuming the simplistic conversion from *H*-band luminosity of Zibetti et al. (2002). These two objects likely have sufficient (∼0.5 mag) *H*-band extinction to bring them above the mass cutoff without assuming a very different mass-to-light ratio. Thus, we have a dilemma: powerful radio sources appear to be able to form in even modestly massive elliptical galaxies (albeit in low numbers), whereas RLQs require a much more luminous host galaxy. Moreover, studies of RLQs and RQQs have generally found a requirement for RLQ host galaxies to be more luminous than their RQQ counterparts (Dunlop et al. 2003; Floyd et al. 2004). Thus, selecting for both optical and radio luminosity results in more luminous host galaxies than *both* selecting for optically luminous objects *and* for radio-luminous ones. There is no obvious reason why either the scattered light (Young et al. 2009) or PSF contamination (Kim et al. 2008) effects should be more significant in RLQs than in RQQs. We therefore echo the conclusion of Best et al. (2005) that radio and optical AGN are separate phenomena.

7. CONCLUSIONS

Here, we again summarize the main findings.

1. In terms of ellipticity, the low-z 3CR are found to be in excellent agreement with Pahre (1999) sample of ellipticals drawn from across a range of environments, and with Floyd and Dunlop quasar samples. The mergers within the 3CR (identified as such in Paper II) fit in well with the general merger population of Rothberg & Joseph (2004).
2. In terms of Sérsic index, there is good agreement with the Floyd et al. quasar and Urry et al. BL Lac object samples, and very poor agreement with the merger population, even when considering just the 3CR mergers in isolation from the remainder of the 3CR sample.
3. In terms of host galaxy luminosity, the 3CR are generally well matched to the Bender et al. (1992); Pahre (1999); and Mobasher et al. (1999) elliptical galaxy samples, but

exhibit far more faint objects than the quasar samples and the BCGs.

4. The Virgo cluster early-type galaxy sample of Ferrarese et al. offers an interesting contrast to the 3CR, clearly illustrating that the latter is drawn from only the most luminous section of a cluster's population.
5. The 3CR and its merging subsample have a similar luminosity range to the mergers of Rothberg & Joseph (2004), but the merging radio galaxies are generally found to be larger, with the Rothberg mergers on the low side of the Kormendy relation.
6. In terms of radio–optical properties, the FR I's in the 3CR unify well with the properties expected of BL Lac objects, and FR II's with RLQs. However, a larger spread is seen in both the morphology and the host galaxy luminosity of the 3CR sources than would be expected from samples of BL Lac objects and RLQs studied so far.

We confirm findings from earlier work (e.g., Ledlow & Owen 1996; Dunlop et al. 2003) that an elliptical host galaxy is a prerequisite for radio-loud AGN activity. However, we identify several radio galaxies (∼20%) that fall below the observed RLQ host galaxy luminosity cutoff at $\sim L^{\star}$. These objects have a luminosity distribution closer to that of the normal elliptical galaxy population, and were missed in the NVSS–6dFGS survey due to the *K*-band flux limit. The same finding is echoed in the morphological comparison—the 3CR host galaxies exhibit a range of Sérsic index that is entirely consistent with the general giant elliptical galaxy population, whereas quasar host galaxies show a narrower range of morphology.

We conclude that the morphological difference is due to quasar selection effects and/or contamination of quasar host galaxy flux by scattered nuclear flux. It would seem highly probable that given accurate coronographic observations, or a higher resolution image of the central regions of quasars, we would observe the same spread in morphologies in the host galaxies of these objects as well. However, we do not believe that the luminosity discrepancy is so easily explained. The fainter FR II host galaxies identified here clearly merit more detailed study and form an interesting subset of the 3CR, containing dusty sources and brightest apparent members small groups.

While we now have a reasonable view of the quasars of host galaxies (and an impressively deep view in a small number of cases—see Bennert et al. 2008), several problems remain. One is the technical issue of separating any scattered nuclear flux from the host galaxy flux. Note that this is distinct from the problem of simply separating out the host galaxy from the PSF. The problem is reviewed by Young et al. (2009) who argue that the effect is likely to affect the measured luminosities of quasar host galaxies significantly. The extent of the problem can be easily tested using space-based optical polarimetry of a bright quasar. The second issue is one of sample bias. Existing quasar host galaxy studies focus on small samples with likely selection biases toward bright host galaxies. We need a statistical survey of low-redshift quasar host galaxies in at least two bands in order to be able to place meaningful constraints on the masses of these objects to provide a baseline against which to compare higher redshift samples.

D.F. acknowledges the support of a Magellan Fellowship from AAL, and the hospitality of OCIW and Las Campanas Observatory during the writing of this paper. We thank Alister Graham for helpful comments on the manuscript and Barry Rothberg and Marc Postman for providing their reduced images and other data. This paper is based on observations with the NASA/ESA *Hubble Space Telescope*, obtained at the Space Telescope Science Institute, which is operated by the Association of Universities for Research in Astronomy, Inc. (AURA), under NASA contract NAS5-26555. This research has made use of the NASA/IPAC Extragalactic Database (NED), which is operated by the Jet Propulsion Laboratory, California Institute of Technology, under contract with the National Aeronautics and Space Administration. We gratefully acknowledge the insightful input of an anonymous referee who made a number of constructive criticisms that significantly improved this paper.

REFERENCES

Allen, M. G., et al. 2002, ApJS, 139, 411
Allington-Smith, J. R., Ellis, R., Zirbel, E. L., & Oemler, A. J. 1993, ApJ, 404, 521
Bender, R., Burstein, D., & Faber, S. M. 1992, ApJ, 399, 462
Bender, R., & Moellenhoff, C. 1987, A&A, 177, 71
Bennert, N., Canalizo, G., Jungwiert, B., Stockton, A., Schweizer, F., Peng, C. Y., & Lacy, M. 2008, ApJ, 677, 846
Best, P. N., Kauffmann, G., Heckman, T. M., Brinchmann, J., Charlot, S., Ivezić, Ž., & White, S. D. M. 2005, MNRAS, 362, 25
Best, P. N., von der Linden, A., Kauffmann, G., Heckman, T. M., & Kaiser, C. R. 2007, MNRAS, 379, 894
Bettoni, D., Falomo, R., Fasano, G., Govoni, F., Salvo, M., & Scarpa, R. 2001, A&A, 380, 471
Bicknell, G. V. 1995, ApJS, 101, 29
Burns, J. O. 1990, AJ, 99, 14
Buttiglione, S., Capetti, A., Celotti, A., Axon, D. J., Chiaberge, M., Macchetto, F. D., & Sparks, W. B. 2009, A&A, 495, 1033
Capaccioli, M., & Caon, N. 1991, R. Astron. Soc., 248, 523
Cohen, M. H., Ogle, P. M., Tran, H. D., Goodrich, R. W., & Miller, J. S. 1999, AJ, 118, 1963
de Koff, S., Baum, S. A., Sparks, W. B., Biretta, J., Golombek, D., Macchetto, F., McCarthy, P., & Miley, G. K. 1996, ApJS, 107, 621
de Koff, S., et al. 2000, ApJS, 129, 33
Disney, M. J., Sparks, W. B., & Wall, J. V. 1984, MNRAS, 206, 899
Donzelli, C. J., Chiaberge, M., Macchetto, F. D., Madrid, J. P., Capetti, A., & Marchesini, D. 2007, ApJ, 667, 780
Dunlop, J. S., McLure, R. J., Kukula, M. J., Baum, S. A., O'Dea, C. P., & Hughes, D. H. 2003, MNRAS, 340, 1095
Emonts, B. H. C., Morganti, R., Oosterloo, T. A., Holt, J., Tadhunter, C. N., van der Hulst, J. M., Ojha, R., & Sadler, E. M. 2008, MNRAS, 387, 197
Fanaroff, B. L., & Riley, J. M. 1974, MNRAS, 167, 31P
Ferrarese, L., et al. 2006, ApJS, 164, 334
Floyd, D. J. E., Kukula, M. J., Dunlop, J. S., Mclure, R. J., Miller, L., Percival, W. J., Baum, S. A., & O'dea, C. P. 2004, MNRAS, 355, 196
Floyd, D. J. E., et al. 2008, ApJS, 177, 148 (Paper II)
Ghisellini, G., & Celotti, A. 2001, A&A, 379, L1
Giovannini, G., Feretti, L., Gregorini, L., & Parma, P. 1988, A&A, 199, 73
Graham, A. W., Erwin, P., Trujillo, I., & Ramos, A. A. 2003, AJ, 125, 2951
Graham, A. W., & Guzmán, R. 2003, AJ, 125, 2936
Graham, A., Lauer, T. R., Colless, M., & Postman, M. 1996, ApJ, 465, 534
Jenkins, C. J., Pooley, G. G., & Riley, J. M. 1977, R. Astron. Soc., 84, 61
Kauffmann, G., et al. 2003, MNRAS, 341, 54
Khochfar, S., & Silk, J. 2006, ApJ, 648, L21
Khochfar, S., & Silk, J. 2009, MNRAS, 397, 506
Kim, M., Ho, L. C., Peng, C. Y., Barth, A. J., & Im, M. 2008, ApJS, 179, 283
Kormendy, J. 1977, ApJ, 218, 333
Kristian, J., Sandage, A., & Katem, B. 1978, ApJ, 219, 803
Lauer, T. R., et al. 1995, AJ, 110, 2622
Ledlow, M. J., & Owen, F. N. 1996, AJ, 112, 9
Ledlow, M. J., Owen, F. N., & Keel, W. C. 1998, ApJ, 495, 227
Ledlow, M. J., Owen, F. N., Yun, M. S., & Hill, J. M. 2001, ApJ, 552, 120
Lilly, S. J., & Longair, M. S. 1984, R. Astron. Soc., 211, 833
Madrid, J. P., et al. 2006, ApJS, 164, 307 (Paper I)
Martel, A. R., et al. 1999, ApJS, 122, 81
Mathis, J. S. 1990, ARA&A, 28, 37
Matthews, T. A., Morgan, W. W., & Schmidt, M. 1964, ApJ, 140, 35
Mauch, T., & Sadler, E. M. 2007, MNRAS, 375, 931
McHardy, I. M. 1974, MNRAS, 169, 527

McLeod, K. K., & McLeod, B. A. 2001, ApJ, 546, 782
McLure, R. J., Kukula, M. J., Dunlop, J. S., Baum, S. A., O'Dea, C. P., & Hughes, D. H. 1999, MNRAS, 308, 377
Milvang-Jensen, B., & Jørgensen, I. 1999, Balt. Astron., 8, 535
Mobasher, B., Guzman, R., Aragon-Salamanca, A., & Zepf, S. 1999, MNRAS, 304, 225
Owen, F. N., & Laing, R. A. 1989, R. Astron. Soc., 238, 357
Owen, F. N., & Ledlow, M. J. 1994, in ASP Conf. Ser. 54, The Physics of Active Galaxies, ed. G. V. Bicknell, M. A. Dopita, & P. J. Quinn (San Francisco, CA: ASP), 319
Pahre, M. A. 1999, ApJS, 124, 127
Perlman, E. S., Stocke, J. T., Carilli, C. L., Sugiho, M., Tashiro, M., Madejski, G., Wang, Q. D., & Conway, J. 2002, AJ, 124, 2401
Postman, M., & Lauer, T. R. 1995, ApJ, 440, 28
Prieto, M. A., Walsh, J. R., Fosbury, R. A. E., & di Serego Alighieri, S. 1993, MNRAS, 263, 10
Privon, G. C., O'Dea, C. P., Baum, S. A., Axon, D. J., Kharb, P., Buchanan, C. L., Sparks, W., & Chiaberge, M. 2008, ApJS, 175, 423
Rothberg, B., & Fischer, J. 2010, ApJ, 712, 318
Rothberg, B., & Joseph, R. D. 2004, AJ, 128, 2098
Schlegel, D. J., Finkbeiner, D. P., & Davis, M. 1998, ApJ, 500, 525
Seigar, M. S., Graham, A. W., & Jerjen, H. 2007, MNRAS, 378, 1575
Simpson, C., Ward, M., Clements, D. L., & Rawlings, S. 1996, MNRAS, 281, 509
Spinrad, H., Marr, J., Aguilar, L., & Djorgovski, S. 1985, PASP, 97, 932
Tadhunter, C. N., Morganti, R., di Serego-Alighieri, S., Fosbury, R. A. E., & Danziger, I. J. 1993, MNRAS, 263, 999
Taylor, G. L., Dunlop, J. S., Hughes, D. H., & Robson, E. I. 1996, MNRAS, 283, 930
Urry, C. M., Scarpa, R., O'Dowd, M., Falomo, R., Pesce, J. E., & Treves, A. 2000, ApJ, 532, 816
Young, S., Axon, D. J., Robinson, A., & Capetti, A. 2009, ApJ, 698, L121
Zakamska, N. L., et al. 2003, AJ, 126, 2125
Zakamska, N. L., et al. 2006, AJ, 132, 1496
Zibetti, S., Gavazzi, G., Scodeggio, M., Franzetti, P., & Boselli, A. 2002, ApJ, 579, 261